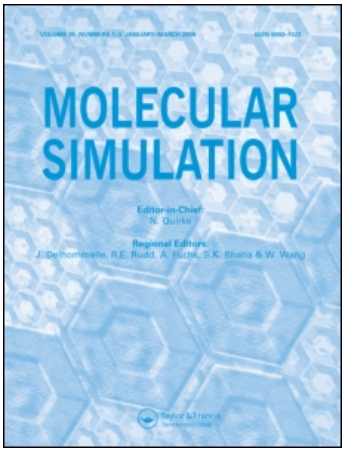

Molecular Simulation
Publication details, including instructions for authors and subscription information:
http://www.informaworld.com/smpp/title~content=t713644482

Influence of Polydispersity and Thermal Exchange on the Flocculation Rate of O/W Emulsions

German Urbina-Villalba[a]; Máximo García-Sucre[a]; Jhoan Toro Mendoza[b]
[a] Centro de Física, Laboratorio de Fisicoquímica de Coloides, Instituto Venezolano de Investigaciones Científicas (IVIC), Caracas, Venezuela [b] Escuela de Física, Facultad de Ciencias, Universidad del Zulia, Maracaibo, Venezuela

Online publication date: 26 October 2010

To cite this Article Urbina-Villalba, German , García-Sucre, Máximo and Mendoza, Jhoan Toro(2003) 'Influence of Polydispersity and Thermal Exchange on the Flocculation Rate of O/W Emulsions', Molecular Simulation, 29: 6, 393 — 404
To link to this Article: DOI: 10.1080/0892702031000117153
URL: http://dx.doi.org/10.1080/0892702031000117153

Molecular Simulation, Vol. 29 (6–7), June 2003, pp. 393–404

Influence of Polydispersity and Thermal Exchange on the Flocculation Rate of O/W Emulsions

GERMAN URBINA-VILLALBA[a,*], MÁXIMO GARCÍA-SUCRE[a] and JHOAN TORO MENDOZA[b]

[a]*Centro de Física, Laboratorio de Fisicoquímica de Coloides, Instituto Venezolano de Investigaciones Científicas (IVIC), Aptdo. 21827, Caracas, Venezuela;* [b]*Escuela de Física, Facultad de Ciencias, Universidad del Zulia, Maracaibo, Venezuela*

(Received July 2002; In final form October 2002)

According to recent simulations [*Langmuir* 16, 7975 (2000)], the flocculation rate (k_f) of concentrated oil in water (O/W) emulsions interacting through van der Waals forces, can reach values considerably higher than the one expected for a very dilute system of non-interacting spheres ($5.49 \times 10^{-18}\,m^3/s$). Similar calculations at a volume fraction $\phi = 0.001$ using 64 particles only, already show a $k_f = 5.83 \times 10^{-18}\,m^3/s$, reasonably close to the theoretical prediction. In this report Brownian Dynamics (BD) simulations are used to study the effect of the volume fraction and the drop size distribution (DSD) on the flocculation rate. First, the dependence of k_f with the maximum value of the thermal interaction between the particles and the solvent is studied. Following, the variation of the flocculation rate is studied as a function of polydispersity for $\phi = 0.15$. As expected, there is a strong dependence of k_f on ϕ. Faster and slower aggregation rates are observed depending on the characteristics of the DSD.

Keywords: Emulsions; Simulations; Coagulation; Brownian dynamics; Coalescence; Flocculation

INTRODUCTION

Almost a century ago Smoluchowski [2] derived a simple formula for the variation of the total number of suspended particles per unit volume n, as a function of time:

$$n = \frac{n_0}{1 + k_f n_0 t} \tag{1}$$

Here, n_0 is the initial particle density, t the time, and k_f a flocculation constant which in the absence of interaction forces is equal to:

$$k_f^{-1} = n_0 t_f = \frac{1}{8\pi a D_0} = \frac{3\eta}{4kT} \tag{2}$$

where η is the solvent viscosity, T the temperature, k Boltzmann constant, t_f a characteristic flocculation time, a the particle radius, and D_0 Stokes diffusion constant equal to:

$$D_0 = \frac{kT}{6\pi\eta a} \tag{3}$$

For water at $T = 298\,K$, t_f is of the order of 2×10^{11} seconds$/n_0$ s [3]. The value of k_f increases in the presence of van der Waals forces and decreases with any kind of repulsive forces like electrostatic, steric, hydrodynamic, etc.

Expressions (1–3) result from an overall mass balance of particle/aggregate collisions of any size leading to either larger or smaller aggregates. Hence, these equations can be used to describe the process of reversible association of colloids (flocculation) as well as the process of irreversible association (coagulation). Coalescence, on the other hand, refers to the merging of two drops to form a unique entity. This additional kind of destabilization can only happen with fluid particles and hence, it is important for emulsions and foams.

According to Verwey and Overbeek [3], Smoluchowski expression for the coagulation rate of lyophobic colloids Eq. (1) can be suitably modified in order to account for short-range repulsive

*Corresponding author. E-mail: guv@ivic.ve

ISSN 0892-7022 print/ISSN 1029-0435 online © 2003 Taylor & Francis Ltd
DOI: 10.1080/0892702031000117153

TABLE I

% Unbalance	Transferred energy (in kT units) $a = 1.0\,\mu m$	Transferred energy (in kT units) $a = 3.9\,\mu m$	Transferred energy (in kT units) $a = 10\,\mu m$
1	15	57	147
5	367	1,432	3,672
10	1,469	5,728	14,688
25	9,180	35,801	91,797
40	23,500	91,650	235,001
50	36,719	143,204	367,189

In order to estimate the energy transfer between solvent molecules and a suspended particle of radius a, the following approximations were made. (a) The maximum number of collisions between a drop and the solvent molecules per unit time was estimated as the ratio between the area of a drop and the cross section of a water molecule. (b) Using the Equipartition Theorem, the velocity and momentum transferred by one water molecule to a drop was calculated ($1/2\,mv^2 = 3/2\,kT$). (c) 1/3rd of the total momentum transferred was assigned to each direction of a coordinate axis. (d) The resulting momentum transferred along a specific axis x, results from the unbalance between the momentum transferred in $+x$ and $-x$ directions, so several percentages of unbalance were tested. (e) The value calculated in (d) divided by the mass of the drop and gives the velocity of the drop along the x axis produced by the thermal exchange. With it, the kinetic energy transferred from the solvent to the drop was computed

barriers and even hydrodynamic interactions (HI) between particles. The effect of such barriers can be incorporated—in average—multiplying Smoluchowski's aggregation velocity by a stability factor W (Fuchs's factor), which in the case of a repulsive barrier between spheres of equal radii (a) is equal to:

$$W = 2a\int_{2a}^{\infty} e^{V/kT}\frac{dR}{R^2} \tag{4}$$

where V is the repulsive potential, and R the distance between two spheres.

In order to prepare a stable colloid that lasts for week or a month ($t_f > 10^6$) prior to coagulation, the stability ratio W have to surpass the value of 10^5 for diluted and 10^9 for very concentrated colloids [3]. Furthermore, since the integrand in Eq. (4) is maximum in the region where V is maximum ($V = V_{max}$), it can also be shown that V_{max} has to be approximately equal to $15\,kT$ for $W = 10^5$, and $25\,kT$ for $W = 10^9$.

The stability considerations that lead to Eq. (4) as well as the estimations of the previous paragraph appropriately consider the effects of Brownian movement on the aggregation rate of a suspension, which is finally accounted for in the formula of k_f through the diffusion constant Eq. (2). However, in the case of emulsions there is an additional contribution: Brownian movement may lead to coalescence at close separations between drops, whenever the momentum transfer between the solvent and the particles at a given time is of the order of the height of their repulsive barrier. That is, coalescence could happen as the result of a "single" irreversible event of the order of a Brownian relaxation time.

Table I shows an order-of-magnitude calculation of the amount of energy that could be transferred from the surrounding water molecules of the solvent to suspended particles of different sizes. These magnitudes are considerably larger than the barrier heights required for preventing aggregation by slowing down the particle diffusion**. This complementary mechanism of destabilization could possibly be related to the findings of Beherens *et al.* [4] regarding the aggregation of charge-stabilized suspensions. According to these authors there is excellent agreement between Derjaguin-Landau-Verwey-Oberbeek (DLVO) theory [3] and experiment, as long as the repulsive barrier is located at least 2 nm away from the particle surface. Sizeable differences occur otherwise. The effect of the momentum transfer on the coalescence rate of emulsions in the presence of a repulsive barrier will be studied in a future report. Here we concentrate on the dependence of the flocculation rate (see below) on the magnitude of the thermal exchange in the absence of a repulsive barrier.

While coagulation and flocculation can be clearly distinguished, there is no precise inter-particle distance to separate the regimes of flocculation and coalescence. Van den Temple [5], for example, suggested that the coalescence rate should be proportional to the number of contacts between flocculated particles. Such assumption implies the existence of finite time between the moment that the particles "touch" and their final unification. Thus, it also supposes the existence of a short-range repulsive barrier and/or a measurable time for draining the intervening liquid between aggregated drops. In Emulsion Stability Simulations (ESS) [1], the particles evolve smoothly until they coalesce. Short-range repulsive barriers have to be explicitly included in the interaction potential. If the particles

**As discussed by Perin [26] and shown by experience, only a fraction of the kinetic energy of a molecule could be transferred. According to a simple estimation from Verwey and Oberbeek [3], the thermal impulse of submicron particles should be usually dissipated in a distance smaller than a typical double layer width.

TABLE II The xx-component of the diagonal elements of the self-diffusion tensor calculated from Batchelor formula [9,10] for a random configuration of particles in a cubic box of side length $12a$ ($a = 3.9 \times 10^{-6}$ m)

Number of particles (radius $= a = 3.9 \times 10^{-6}$ m)	*Volume fraction* ($\phi \times 100$)	D_{11}^{xx}/D_0
1	0.236	1.000
5	1.18	0.996
34	8.00	0.932
64	15.1	0.867
125	29.6	0.579
216	51.0	0.227

coalesce immediately after their surfaces get into contact, coalescence is then "included" in the flocculation rate, that is: $k_f = k_{co}$. Drops increase their size as they collide in a similar way as suspended solid particles form bigger aggregates upon collisions. In presence of a short-range barrier, the coalescence rate can be neatly estimated by comparing the resulting flocculation rate with its respective value in the absence of such barrier.

Since the formulation of Eq. (1), several improvements of this simple formula were published [5–7]. Some approaches reconsider the analytical description of the process of flocculation only [6], while some others explicitly introduce the coalescence rate [5,7]. Up to our knowledge all related developments depart from a mono-dispersed system of evenly distributed particles, which evolves with time. However, the initial drop size distribution (DSD) of a typical emulsion is almost invariably polydisperse and spatially inhomogeneous just after preparation. The question we wish to address in the second part of this communication is: what is the effect of that initial polydisperse distribution on the aggregation rate?

In order to quantify the effects of polydispersity on the coalescence rate it is necessary to separate the effect of the volume fraction (ϕ) from that of the DSD. Both, ϕ and DSD affect k_f through the dependence of the diffusion tensor of the drops on (a) the radii of the particles; (b) their distribution in space; and (c) the variation of the inter-particle potential with the average distance and radii of the drops [8]. Points (a) and (b) can be illustrated by calculating the variation of the xx component of the self-diffusion D_{11} tensor of a particle of radius $a = 3.9$ μm subject to different environments. Table II shows the value of D_{11}^{xx} when the particle is immersed in distinct sets of similar particles randomly distributed in a cubic box of side length of 12.1 a with periodic boundary conditions. The expression of D_{11}^{xx} used includes hydrodynamic corrections from Batchelor [9–10]. As expected, D_{11}^{xx} decreases as the volume fraction increases. Table III shows similar calculations employing 64, 125 and 216 particles. Here the volume fraction is maintained at $\phi = 0.15$, but different distributions of radii between 0.1 a and 1.0 a are used. It is clear that D_{11}^{xx} also changes with the characteristics of the DSD employed. Furthermore, at fixed ϕ, D_{11}^{xx} also depends on the initial configuration of the particles (Table III). It is clear then that HI [11–15] mix the effects of ϕ and DSD on the flocculation rate due to their influence on the diffusion [D_{ij}]. HI are also known to decrease the aggregation rate considerably [12], and favor the formation of open structures of clusters of particles instead of "globular" ones [15].

Averaging mobility functions $[b_{ij}] = kT/[D_{ij}]$ over two-particle and three-particle distribution functions lead to analytical expressions for the variation of the diffusion constant of *monodisperse* systems with the volume fraction, $D(\phi)$ [10,16–19] at three levels of approximation:

$$D(\phi) = D_0[1 - 1.83\phi + \cdots] \quad (5)$$

$$D(\phi) = D_0[1 - 1.73\phi + \cdots] \quad (6)$$

$$D(\phi) = D_0[1 - 1.73\phi + 0.93\phi^2 + 1.80\phi^3 + \cdots] \quad (7)$$

For times t greater that a Brownian relaxation time $\tau_B = MD/kT$ (where M is the mass of the particle), but considerably smaller than the time required to diffuse a mean inter-particle distance,

TABLE III Similar calculations to those of Table I for a poly-disperse distribution of particles: (O) uniformly spaced throughout the simulation box, or (R) randomly distributed

Number of particles	*Ordered (O) Or Random (R)*	*Volume fraction* ($\phi \times 100$)	*DSD # particles* × *radius* ($a = 3.9 \times 10^{-6}$ *m*)	D_{11}^{xx}/D_0
64	O	15.13	$64 \times 1\ a$	0.8499
64	R	15.13	$64 \times 1\ a$	0.8678
125	O	15.14	$21 \times 0.1\ a$ $51 \times 0.6\ a$ $53 \times 1.0\ a$	0.6841
125	R	15.14	$21 \times 0.1\ a$ $51 \times 0.6\ a$ $53 \times 1.0\ a$	0.8199
216	O	15.11	$22 \times 1.0\ a$ $194 \times 0.6\ a$	0.5834
216	R	15.11	$22 \times 1.0\ a$ $194 \times 0.6\ a$	0.7981

$\tau_I = n^{-2/3}/D$ ($\tau_B \ll t \ll \tau_I$) [18], the effects of direct interaction forces are small [20–24]. In this regime, it is found that the particles diffuse with a short-time self-diffusion coefficients D^s. Formulae (5)–(7) were calculated employing a hard-sphere radial distribution function and the hydrodynamic tensors of Batchelor [10] and Felderhof [16]. These expressions correspond to the short-time regime, where $D = D^s$ [24].

As expected from both theory and experiment [25–27], D^s is proportional to the mean square displacement of a particle $\langle[\Delta r(t)]^2\rangle$ in systems of non-interacting colloids [24]. However, for intermediate times of the order of a^2/D, that is no longer the case. In spite of this it is found that whenever $t \gg \tau_I$, $\langle[\Delta r(t)]^2\rangle$ becomes again proportional to time but with a different diffusion constant (D^L) [24].

As shown by van Veluwen *et al.* [24] short time self-diffusion coefficients can be measured by dynamic light scattering using monodisperse samples of large particles ($a \geq 0.4\,\mu m$). The theory of Beenakker and Mazur [28] based on the partial summation of many-body HI reproduces experimental data on 0.4-μm silica particles up to $\phi = 0.20$ with only slight deviations. However, higher order approximations are necessary for higher volume fractions of the internal phase. These results are consistent with Photon Correlation Spectroscopy measurement [19], which demonstrates that Eqs. (5)–(7) cannot account for the true value of the effective diffusion constant at $\phi \geq 0.3$ due to the presence of many-body HI.

COMPUTATIONAL DETAILS

Thermal Exchange

Recently several new computational techniques [29–31] as well as new algorithms for Brownian dynamics (BD) simulations appeared [32–37]. Although different methodologies seem to be very promising in handling of a large number of particles [29], BD has proved to be very successful in capturing those microscopic details, which are essential to colloidal stability [38–44]. This is critical in those cases where the kinetics of adsorption of molecules to the interface determines the interaction potential [41,45]. On the other hand, one of the major disadvantages of the BD technique is the small time step required in order to sample appropriately the interaction potential between particles.

According to the algorithm of Ermak and McCammon [46] the position of a Brownian particle at time $(i+1)\Delta t$ along a given coordinate axis (X) equals its previous position at time $i\Delta t$ plus a steady diffusive contribution and a random term R_i: In the absence of long-range fluid-mediated hydrodynamic coupling:

$$X_{i+1} = X_i + \left(\frac{DF}{kT}\right)\Delta t + R_i \tag{8}$$

where D is the diffusion constant, F the total force acting on the particle.

Most calculations presented were run under the action of thermal interaction only ($F = 0$). Whenever van der Waals forces were considered, Hamaker expression for the potential energy (V) between spheres of different size was used:

$$V = -\frac{A}{12}\left[\frac{y}{x^2+xy+x} + \frac{y}{x^2+xy+x+y} + 2\ln\left(\frac{x^2+xy+x}{x^2+xy+x+y}\right)\right] \tag{9}$$

where A is the Hamaker constant, $x = d/2R_1$, $y = R_2/R_1$, and "d" is the shortest distance between the particles.

In practical terms, every random displacement R_i in Eq. (8) is calculated by multiplying a real number sampled from a Gaussian distribution of zero mean and unit variance by $[2D\Delta t]^{1/2}$. In the absence of a steady force ($F = 0$), these procedures lead to $\langle[\Delta x(t)]^2\rangle = 2D\,\Delta t$ and $\langle[\Delta r(t)]^2\rangle = 6D\,\Delta t$ as experimentally observed in dilute systems [25–27]. In principle, any single displacement length is possible [47–48] as long as the set of displacements reproduces the statistical properties of a Gaussian distribution. Table IV shows some statistical properties of the Gaussian Routine used in these calculations [49]. First, it can be seen that the code appropriately reproduces the theoretical properties of a Gaussian function (columns 3, and 4–6). The average value comes out very close to zero in all cases. The random number generator employed can produce values as high as 6.0 units for a 600-million sample. According to the statistics, the random displacement in a single move will be higher than $[6D\,\Delta t]^{1/2}$ as much as 31% of the time.

Although the time-average thermal exchange between colloidal particles and their suspending media is of the order of kT, the energy transmitted in a single event of the order of a Brownian relaxation time could be much higher. In BD simulations the average thermal exchange is usually controlled through the selection of the time step, which is also limited by the width of the repulsive barrier. Since the particles should sample the potential appropriately, a high repulsive barrier should prevent coalescence in the absence of the thermal interaction. This means that the maximum displacement of a particle at a given time-step should be a fraction of the repulsive barrier width.

In order to study the effect of the thermal interaction on the flocculation rate (in conditions

TABLE IV Some mathematical properties of the random number generator (Box-Muller) used in the present work.

Multiples (M) of the Standard Deviation (σ) Mσ*	*Theoretical percentage of values above M*σ*	*Number of iterations of the random generator*	*% X*	*% Y*	*% Z*	*Maximum value*	*Minimum value*
1.0 σ	31.74	1.0×10^4	32.51	32.06	31.30	4.2129	− 4.3056
1.0 σ	31.74	1.0×10^5	31.85	31.55	31.76	4.7843	− 4.5367
1.0 σ	31.74	1.0×10^6	31.74	31.70	31.77	5.2184	− 5.0894
1.0 σ	31.74	1.0×10^7	31.73	31.74	31.74	5.5176	− 5.2886
1.0 σ	31.74	1.0×10^8	31.73	31.73	31.73	5.8554	− 5.8653
1.0 σ	31.74	6.0×10^8	31.73	31.73	31.73	5.8554	− 6.0608
0.5 σ	62.00	1.0×10^6	61.66	61.67	61.79	5.2184	− 5.0895
1.0 σ	31.74	1.0×10^6	31.74	31.70	31.77	5.2184	− 5.0895
2.5 σ	1.24	1.0×10^6	1.24	1.23	1.26	5.2184	− 5.0895
3.9 σ	0.00	1.0×10^6	0.009	0.012	0.010	5.2184	− 5.0895

The maximum values obtained for a given set of generated numbers (iterations) are shown, along with the probability of obtaining a number higher than a given multiple of standard deviations (σ) from the average. Every sampling includes values for three variables x, y, z. Thus the total sample is really three times the value of column 3. The maximum and minimum values reported are the absolute maximum and minimum values that result from the comparison of x, y and z values

for which $k_f = k_{co}$), we implemented a routine that calculates the kinetic energy ($1/2\,mv^2$) gained by the particle after a random kick. For this purpose, the velocity of a particle in each axis was calculated by dividing its random displacement along that direction, by the time step. The value of the kinetic energy was then compared to a pre-selected threshold. Random displacements were only accepted if they came out to be lower than the given threshold. The use of a "maximum supremum" was already suggested by Bacon *et al.* [39] in a footnote of their seminal work regarding the motion of flocs composed of two and three particles. It was indicated that this technique could prevent solid particles from overlapping during the course of the simulation. By passing we note that one of the main results of that research is that the particles can "jump" out of potential well of depth $10\,kT$ within a matter of seconds.

In this work two distinct thresholds are used, namely 100 and 10,000 kT. Additional 10-kT calculations are also presented. As the simulation evolves the particles are allowed to coalesce. In this case a new particle appears at the position of the center of mass of the colliding particles, and the diffusion constant is recalculated for the new radius according to Stokes law Eq. (3). From the variation of the number of particles per unit volume "n" vs. time, the half-life time was evaluated. The coalescence rate was calculated first adjusting k_f in Eq. (1), until the sum of the square differences between the values of n given by the simulation and calculated according to Eq. (1) was minimized. Additionally, the minimum square method (MSM) was used to calculate the slope of the curve $1/n$ vs. t (see Eq. (1)), which directly yields the referred rate.

Polydispersity

Similar calculations to those previously described were run over polydispersed systems (Table V) of particles. Since there are infinite ways to distribute

TABLE V Drop size distributions employed in the simulations

ID	ϕ ($\times 100$)	*r/a* 2.0	*r/a* 1.5	*r/a* 1.2	*r/a* 1.1	*r/a* 1.0	*r/a* 0.9	*r/a* 0.8	*r/a* 0.7	*r/a* 0.6	*r/a* 0.5	*r/a* 0.4	*r/a* 0.3	*r/a* 0.2	*r/a* 0.1
1	1.14									4	15	26	15	4	
2	2.24								1	12	52	86	52	12	1
3	5.39							2	16	45	44	16	2		
4	9.33							4	28	76	76	28	4		
5	12.59							35	43	60	43	35			
6	15.11					20	1	61	21	22					
7	15.11					22	0	0	0	194					
8	15.13					21	21	21	21	22	22	22	22	22	22
9	15.13					64									
10	15.13					52	0	0	0	55	0	0	0	0	109
11	15.70					7	30	50	30	7	1				
12	15.97		20	0	0	0	0	0	0	0	0	0	0	0	44
13	22.29				7	30	51	30	7						
14	29.50	9	11	9	0	0	0	0	0	0	0	0	0	0	96
15	29.56					125									
16	29.57					114	0	0	0	51	0	0	0	0	51
17	30.38			7	30	51	30	7							
18	51.07					216									

TABLE VI Slope of the curve $\langle(\Delta r^*(t))^2\rangle$ vs. t^* for several thresholds. The scaled displacement and time are equal to $(r^*)^2 = (r/a)^2$ and $t^* = (t\,D/a^2)$, respectively.

Slope $\langle(\Delta r^*)^2\rangle$ *vs.* t^*	*Threshold (in k T units)*	*Diffusion tensor used*	*Radius (a)*
12.01	10,000	Stokes	$r = 1.95 \times 10^{-6}$
6.00	10,000	Stokes	$r = 3.90 \times 10^{-6}$
3.00	10,000	Stokes	$r = 7.80 \times 10^{-6}$
12.01	100	Stokes	$r = 1.95 \times 10^{-6}$
5.66	100	Stokes	$r = 3.90 \times 10^{-6}$
1.29	100	Stokes	$r = 7.80 \times 10^{-6}$
3.00	10,000	Batchelor	$r = 7.80 \times 10^{-6}$
2.94	1000	Batchelor	$r = 7.80 \times 10^{-6}$
0.70	100	Batchelor	$r = 7.80 \times 10^{-6}$

In the absence of other particles and under Stokes dynamics, the slope corresponding to $a = 3.9 \times 10^{-6}$ should be equal to 6.00.

these particles amongst a cubic box, the average distance between particles may change artificially as a function of the initial configuration. For this reason all calculations with the same number of particles departed from the same random positions, regardless of their DSD. The present calculations are meant to serve as standards for more involved simulations in which short-range repulsive barriers are considered [1,45,50–51]. As in our previous simulations regarding the stability of Bitumen emulsions, we use here a small number of particles (64, 125, 216).

For most calculations a time step (Δt) equal to 1.36×10^{-6} s was used. For volume fractions (ϕ) of 0.001, 0.01 and 0.08, time steps of 1.36×10^{-2}, 1.36×10^{-4} and 3.4×10^{-6} s, were used. Despite the very large time step required for $\phi = 0.001$, the value of k_f calculated was $5.83 \times 10^{-18}\,m^3/s$, in reasonable agreement with the theoretical estimate Eq. (2) $5.49 \times 10^{-18}\,m^3/s$. Using a similar technique based on the probability density function of random displacements [34], Puertas obtained a value of $6.16 \times 10^{-18}\,m^3/s$ ($\Delta t = 1 \times 10^{-4}$ s). It should be kept in mind that the algorithm used [46] to simulate the Brownian movement, corresponds to the regime in time where the mean square displacement of the particle is proportional to the time [48]. For a particle of 3.9 μm, this corresponds to times larger than $\tau_B = 3.38 \times 10^{-6}$ s. Only after several iterations this requirement is met, but for one individual movement the Δt used is lower than the Brownian relaxation time. More accurate algorithms for these cases are also available [52]. As demonstrated by the value of k_f ($\phi = 0.001$), it is unlikely that this simplification sensibly affect the aggregation rates. However, its suitability especially for the cases where surfactant adsorption is considered, is still under study.

RESULTS AND DISCUSSION

Table VI shows the value of the diffusion constant of a particle evaluated from its mean square displacement for various magnitudes of thermal threshold. It is clear that in order to reproduce the experimental value found in dilute systems [25–27], high values of the thermal threshold must be considered. At $100\,kT$ significant deviations are already observed. These appear to increase with the increase of the particle radius. The effect is more pronounced whenever HI are considered.

Figure 1 shows the variation of the flocculation half time $t_{1/2} = t(n_0/2)$ with the volume fraction, for different values of the thermal threshold (U_T). The corresponding values $t_{1/2}$ and k_f are shown in Table VII. In order to visualize the results a logarithmic scale was used. First, it becomes clear that the predicted half times using Smoluchowski's formula Eq. (2) are rather long. That formula sensibly overestimates the stability of the emulsion for all volume fractions higher than $\phi = 0.01$. At $\phi = 0.001$, the curves of 10, 100 and $10{,}000\,kT$ converge. Taking into account the limited amount of volume fractions probed, it appears that the differences in $t_{1/2}$ due to the thermal threshold are not very large for $\phi \leq 0.15$.

Figure 1 also shows the results of the analytical formula proposed by Hütter [53] for a suspension of Al_2O_3 particles ($a = 0.5\,\mu m$) stabilized by electrostatic barriers lower than $6\,kT$:

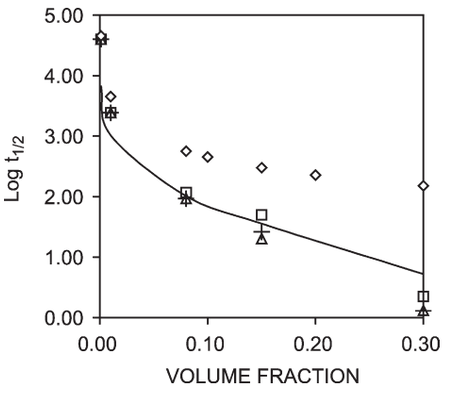

FIGURE 1 Logarithm of the half-life time as a function of the volume fraction for 3.9-μm Brownian particles using several thermal thresholds: (□) $U_T = 10\,kT$, (+), $U_T = 100\,kT$, (Δ) $U_T = 10{,}000\,kT$). The predictions of Eqs. (1) (◇) and (10) (−) are also shown.

TABLE VII Half-life times and flocculation constants for $U_{T=}10\,kT$, $100\,kT$ and $10{,}000\,kT$, as a function of the volume fraction of oil

ϕ	k_f (m^3/s) $10\,kT$	k_f (m^3/s) $100\,kT$	k_f (m^3/s) $10{,}000\,kT$	$t_{1/2}$ (s) $10\,kT$	$t_{1/2}$ (s) $100\,kT$	$t_{1/2}$ (s) $10{,}000\,kT$
0.001	5.83×10^{-18}	5.83×10^{-18}	5.83×10^{-18}	40,003	40,003	40,003
0.01	1.02×10^{-17}	1.02×10^{-17}	1.02×10^{-17}	2,435	2,435	2,435
0.08	2.47×10^{-17}	3.22×10^{-17}	3.22×10^{-17}	117.2	92.4	92.4
0.15	3.37×10^{-17}	5.52×10^{-17}	7.16×10^{-17}	49.8	26.2	20.2
0.30	2.77×10^{-16}	1.77×10^{-16}	8.41×10^{-17}	2.24	1.29	1.3

$$t_{1/2} = \alpha_1 \left[\sqrt[3]{\frac{\phi_m}{\phi}} - 1 \right]^{\alpha_2} \tag{10}$$

The parameters corresponding to aluminum oxide for a vanishing value of the surface potential are [53]: $\alpha_1 = 3.3\times10^{-2}$, $\alpha_2 = 2.23$, $\phi_m = 0.479$. A reasonable fit of Eq. (10) to the present data corresponds to the values: $\alpha_1 = 1.4\times10^{+2}$, $\alpha_2 = 2.00$, $\phi_m = 0.51$ (cubic packing). The value of α_1 is considerably larger than that of Ref. [53] for the same volume fractions, but the number of particles per unit volume in that case is considerably higher ($t_{1/2} = 1/k\,n_0$ according to Eq. (1)). It should also be noticed that Eq. (10) is used in Ref. [53] to measure the time after which the number of *free* particles has dropped to half of its initial value. The data of Figs. 1 and 2 correspond to times for which the *total* number of particles in the system drops is reduced in 50%.

Figure 2 (Table VIII) shows a complementary set of calculations on monodispersed systems of particles interacting through van der Waals attraction. The variation of the half lifetime for the original values of α_1 α_2 at $\phi_m = 0.51$ is shown there for further reference. In this calculation $U_T = 10,000\,kT$, and Hamaker constants of 1.24×10^{-19}, 1.24×10^{-20} and 1.24×10^{-21} were used. As before, all computations converge at low volume fractions. For the present DSD, it is further observed that the use of a Hamaker constant of 1.24×10^{-21} originates half lifetimes very similar to those of systems of non-interacting particles executing random walks.

Figure 3 shows the dependence of k_f as a function of the volume fraction for $U_T = 10$, 100 and $10{,}000\,kT$. Curve identified as "unbound" in this figure refers to the flocculation constant obtained in the absence of a restriction to the thermal threshold. At $\phi < 0.15$ there is a slight dependence of the flocculation constant on the thermal threshold. However the dependence is very pronounced for $\phi > 0.15$. Thus, measurements of k_f at these concentrations could be used to estimate the magnitude of the thermal interaction in concentrated emulsions. The values of k_f listed in the Tables correspond to the slope of the curve of $1/n$ vs. t (Procedure A). The flocculation constants computed by minimization of the total difference between the calculated and the simulated number of particles at each time (Procedure B) showed a less smooth monotonous variation with the increase of the volume fraction. These differences are expected to diminish as the number of particles in the simulation is increased. While Procedure A makes more emphasis in the first steps of the simulation, Procedure B weights the overall curvature of k_f vs. t, including long times for which the number of particles is very small.

Figure 4 shows the variation of the number of particles per unit volume for a selected set of polydisperse systems using a maximum threshold

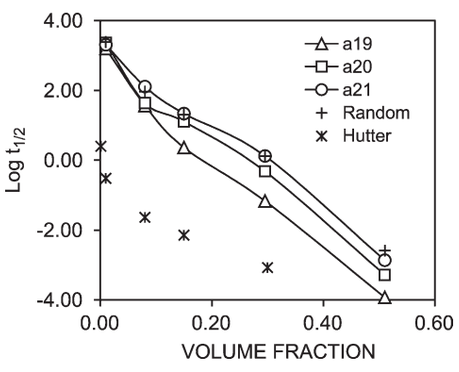

FIGURE 2 Logarithm of the half-life time as a function of the volume fraction for Brownian particles interacting through van der Waals forces at $U_T = 10,000\,kT$. Results for Hamaker constants of 1.24×10^{-19}, 1.24×10^{-20} and 1.24×10^{-21} are shown.

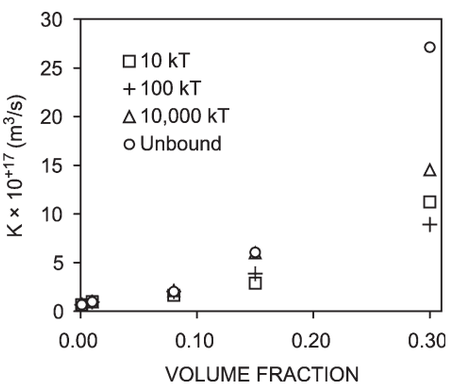

FIGURE 3 Dependence of the flocculation rate of monodispersed systems of non-interacting particles as a function of the volume fraction for different magnitudes of U_T (see Table VII).

TABLE VIII Half-life times and flocculation constants for three order of magnitude of the Hamaker constant: 1.24×10^{-19} J, 1.24×10^{-20} J, 1.24×10^{-21} J, as a function of ϕ for fixed $U_T = 10,000\,kT$

ϕ	k_f (m^3/s) $A = 1.24\times10^{-19}$ J	k_f (m^3/s) $A = 1.24\times10^{-20}$ J	k_f (m^3/s) $A = 1.24\times10^{-21}$ J	$t_{1/2}$ (s) $A = 1.24\times10^{-19}$ J	$t_{1/2}$ (s) $A = 1.24\times10^{-20}$ J	$t_{1/2}$ (s) $A = 1.24\times10^{-21}$ J
0.01	1.38×10^{-17}	7.49×10^{-18}	8.91×10^{-18}	1,568	2,312	2,025
0.08	6.28×10^{-17}	3.21×10^{-17}	2.02×10^{-17}	36.9	43.5	128.7
0.15	1.70×10^{-16}	6.82×10^{-17}	3.65×10^{-17}	2.3	12.7	21.7
0.30	6.82×10^{-15}	5.95×10^{-16}	3.30×10^{-16}	0.07	0.48	1.33
0.51	7.23×10^{-11}	6.25×10^{-12}	1.26×10^{-12}	1.19×10^{-4}	5.19×10^{-4}	1.37×10^{-3}

of $100\,kT$. The related data along with a set of calculations carried out at $U_T = 10,000\,kT$ are shown in Table IX. It is observed that despite the differences in initial number of particles the slope of the curves is similar. Thus, the flocculation constant comes out to be of the same order of magnitude, although there is a clear dependence on polydispersity. Such differences are more pronounced for half-life times evaluated directly from the simulation data.

Figure 5 shows the variation of the number of particles per unit volume as a function of time for systems of equal number of particles but variable volume fraction. In order to appreciate the differences between the calculations only a section of the curves is shown. As expected, emulsion destabilization becomes more pronounced as the volume fraction increases. The curves show different slopes corresponding to distinct flocculation rates.

Figure 6 shows the dependence of k_f on the volume fraction. Here the effect of polydispersity at $\phi = 0.15$ ($U_T = 100\,kT$) can be clearly observed. According to the present results, the rate constant at $\phi = 0.15$, can vary as much as 2.2 times as a consequence of polydispersity only. A more pronounced effect is observed with respect to the volume fraction. Changing ϕ from 0.001 to 0.16 may increase the rate constant in one order of magnitude depending on polydispersity, while a change in ϕ from 0.15 to 0.30 speeds up phase separation in one additional order of magnitude. At $U_T = 10,000\,kT$, the combined effect of increasing the volume fraction from $\phi = 0.001$ to 0.30, and changing the polydispersity of the system, may increase the flocculation constant in only 53 times.

Figure 7 shows the variation of the half lifetime for polydisperse systems ($U_T = 100\,kT$). The values predicted by Eq. (10) for $\alpha_1 = 24$, $\alpha_2 = 2.0$ and $\phi_m = 0.51$ are also shown. The agreement is good considering the limited amount of small-particle simulations presented. Comparison of this value of α_1 with that previously obtained for monodisperse systems indicate that this constant may drastically change as a function of the DSD. This is reasonable since Eq. (10) is derived from an estimation of the mean free path between the particles, that changes with the number and radii of the particles in the system.

The effect of the interaction potential on the flocculation rate including HI will be addressed in a future communication. However, in order to illustrate the effect that those variables may have on the flocculation rate, the results of additional 125-particle simulations ($a = 3.9\,\mu$m) at $\phi = 0.15$ are also presented (Fig. 8(a),(b)). Here, only the points where the number of particles changes as a function of time are illustrated. At $\phi = 0.15$ the thermal movement of the particles produces a value of $k_f = 2.91\times10^{-17}$ m^3/s ($r^2 = 0.9856$). However when van der Waals (vdW) attraction is included (Hamaker constant $= 1.24\times10^{-19}$), $1/n$ is only linear in one portion of the curve. The rate constant evaluated in that linear portion is 2.7 times higher, $k_f = 7.78\times10^{-17}$ m^3/s ($r^2 = 0.9560$). Hydrodynamic interactions, on the other hand, set a limit to the

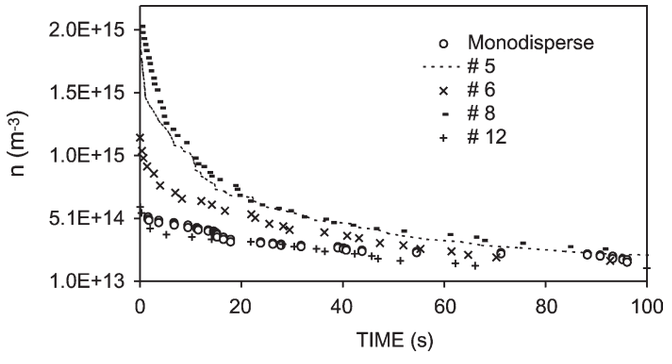

FIGURE 4 Evolution of the number of particles per unit volume (n) as a function of time, for different DSDs of similar volume fraction $\phi \sim 0.15$. The identification of the DSD is shown in the legend (see Table V).

TABLE IX Half-life times and flocculation constants for systems of polydispersed particles as a function of ϕ and U_T with emphasis in $U_{T=}100\,kT$

ID	$\phi \times 100$	$k_f\,(m^3/s)\ 100\,kT$	$t_{1/2}$ (s) $100\,kT$	k_f (m^3/s) $10{,}000\,kT$	$t_{1/2}$ (s) $10{,}000\,kT$
1	1.11	7.49×10^{-18}	154.2	7.61×10^{-18}	154.2
2	2.24	1.17×10^{-17}	79.1	1.02×10^{-17}	81.4
3	5.39	1.17×10^{-17}	67.0	1.35×10^{-17}	70.9
4	9.33	2.42×10^{-17}	11.6	1.72×10^{-17}	15.0
5	12.59	3.76×10^{-17}	9.4	2.99×10^{-17}	7.7
6	15.11	5.10×10^{-17}	16.0	3.01×10^{-17}	11.9
7	15.11	3.12×10^{-17}	6.6	3.46×10^{-17}	6.5
8	15.12	3.52×10^{-17}	9.7	4.49×10^{-17}	10.0
9	15.13	3.86×10^{-17}	26.2	6.00×10^{-17}	20.2
10	15.13	3.94×10^{-17}	8.05	4.06×10^{-17}	6.3
11	15.70	3.21×10^{-17}	24.2	2.75×10^{-17}	23.2
12	15.97	7.39×10^{-17}	24.3	4.22×10^{-17}	27.8
13	22.29	6.88×10^{-17}	10.1	6.13×10^{-17}	8.3
14	29.50	1.37×10^{-16}	4.35	1.40×10^{-16}	5.7
15	29.56	8.91×10^{-16}	1.29	1.45×10^{-16}	1.3
16	29.57	1.36×10^{-16}	0.78	1.76×10^{-16}	0.5
17	30.38	5.53×10^{-16}	1.2	4.05×10^{-16}	1.9

acceleration produced by the van der Waals interaction. HI slow down the flocculation rate producing an intermediate result: $k_f = 4.48 \times 10^{-17}\,m^3/s$ ($r^2 = 0.9720$), roughly 0.5 times slower than the vdW rate. This number is consistent with the decrease of the coagulation time due to HI, previously calculated by Bacon *et al.* [39]: 2.5 times for particles of 0.5–1.0 μm interacting through DLVO forces at $\phi = 0.155$. Figure 8(b) shows again the combined effect of the van der Waals attraction and the HI. In these calculations and some other unpublished simulations, we have found that the vdW + HI effect, usually produces a flocculation constant ($3.07 \times 10^{-16}\,m^3/s$) that does not differ very much from the random walk evaluation. As a matter of fact, the difference between the vdW + HI value and the thermal one ($1.72 \times 10^{-16}\,m^3/s$) for this case ($\phi = 0.30$) is considerably smaller than the deviations originated by polydispersity as was previously illustrated.

It is important to stress here that in the presence of inter-particle interactions (and for the small number of particles used) the simulation data shows large deviations from linearity at very long times. In the absence of inter-particle forces, the variation of $1/n$ vs. t is linear for more than 85% of the total simulated time (see Table X). In those cases deviations from linearity arise when the number of drops diminishes considerably until only a few remain. When other inter-particle forces are included, the variation of $1/n$ vs. t, which appears to be roughly linear according to Fig. 8, also deviates considerably at short times. This figure was purposely chosen in order to illustrate that the presence of an interaction force can extend the very small transient observed in thermal simulations prior to the linear behavior. This anomaly is a function of the number of particles, their initial configuration, polydispersity and also the thermal threshold. Higher U_T values, number of particles, and usually—but not always—polydispersity, appear to decrease the transient region. No other conclusions can be derived from the calculated data at this point.

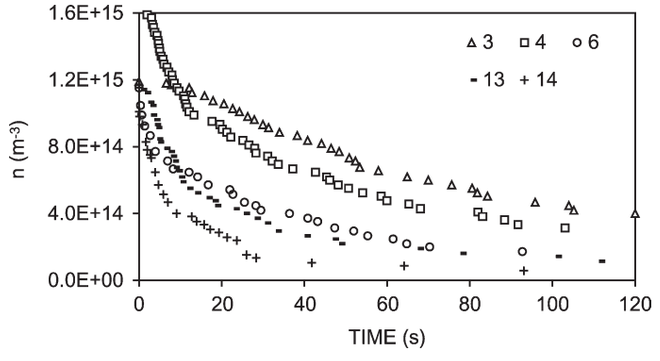

FIGURE 5 Variation of n vs. t for polydisperse systems of 125 particles ($U_T = 100\,kT$), as a function of the volume fraction of the internal phase. The numbers in the legend correspond to the system identifications shown in Table V.

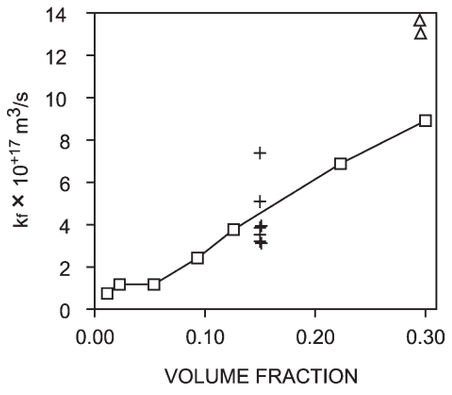

FIGURE 6 Dependence of the flocculation rate on the volume fraction of internal phase for $0.01 < \phi < 0.30$. The crosses (×) indicate the results obtained for the polydisperse systems specified in Table V for $\phi = 0.15$. The triangles (Δ) correspond to the set of polydisperse systems specified in Table V for $\phi = 0.30$.

Neglect of HI causes an overestimation of k_f. However, appropriate account of HI in concentrated systems is difficult due to the intrinsic "many-body" nature of this effect. For the calculations of Fig. 8, pairwise additive HI were assumed. It is known that this assumption breaks down in concentrated emulsions due to the screening of the HI by intervening particles [56].

One important consequence of comparing the flocculation rates successively evaluated with: (a) thermal interaction only (T), (b) T + vdW and (c) T + vdW + HI, relates to the appropriate computation of the stability ratio W Eq. (4). As formerly shown by Fuchs [3,57], the value of k_f in the presence of a repulsive barrier (or HI) is equal to $k_f = k_0/W$, where k_0 is the fast flocculation rate. However, it is observed that the flocculation rate evaluated for case (c) can be faster than that for case (a) due to the van der Waals attraction. Thus, k_0 does not refer to the thermal (random walk) case as one may initially assume following Smoluchowski approach. It does refer to the value of k_f in the absence of a repulsive barrier, which *includes vdW attraction*, as correctly assumed in experimental evaluations [55] of k_f.

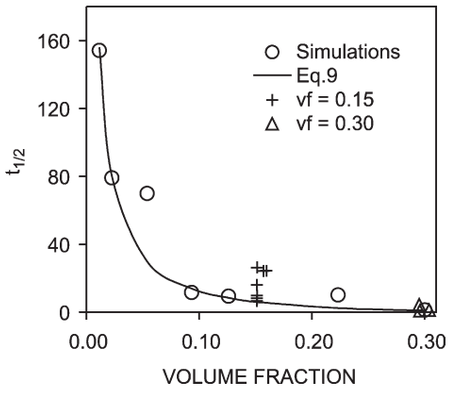

FIGURE 7 Dependence of the half lifetime as a function of the volume fraction for the polydisperse systems of Table V at $U_T = 100\,kT$. The crosses (×) correspond to $\phi = 0.15$ simulations, while the triangles (Δ) correspond to $\phi = 0.30$ calculations.

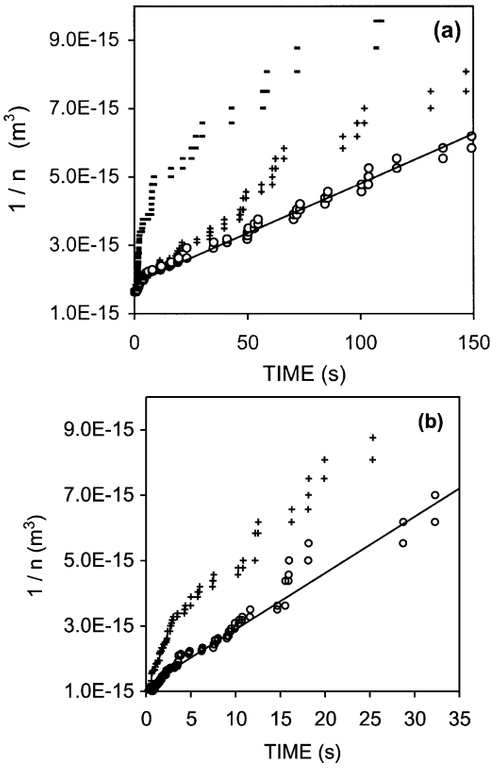

FIGURE 8 Variation of $1/n$ vs. t at $\phi = 0.15$, $U_T = 10\,kT$ for a set of 64 particles moving under the influence of: (○) thermal exchange with the solvent; (−) thermal interactions plus van der Waals forces; (+) both thermal and vdW forces with an approximate account of hydrodynamic interactions ($\phi = 0.15$) [12]. Results for $\phi = 0.15$ and $\phi = 0.30$ are shown in Fig. 8(a),(b) respectively. Approximate hydrodynamic interactions were computed assuming pair-wise additive hydrodynamic forces. An alternative cluster model for HI along with a discussion regarding artifacts caused by the neglect of many-body interactions on the diffusion tensor can be found in Refs. [38,39].

CONCLUSIONS

Coagulation constants of emulsions are usually very difficult to measure not only due to technical problems but also due to the multiple coupled mechanisms of emulsion de-stabilization that simultaneously occur in a typical system. Except for a few direct microscopic observations on the behavior of a limited number of particles reported many years ago [26–28], very few publications address this problem [54], and most of them deal with the flocculation of two particles. Only recently, a light scattering technique suitable for the evaluation of coagulation constants has been reported [55]. By that mean it has been possible to confirm the applicability of Eq. (1)

TABLE X Flocculation rates calculated for the systems of Table V, including a van der Waals interaction with a Hamaker constant equal to 1.24×10^{-19} J

ID	$\phi \times 100$	*Number of particles*	k_f (m^3/s) 10,000 kT	$t_{1/2}$ (s) 10,000 kT
1	1.11	64	1.05×10^{-17}	75.1
2	2.24	125	1.67×10^{-17}	60.2
3	5.39	125	3.22×10^{-17}	32.3
4	9.33	216	8.62×10^{-17}	1.8
5	12.59	216	1.10×10^{-16}	0.58
6	15.11	125	3.01×10^{-16}	1.2
7	15.11	216	1.32×10^{-16}	0.5
8	15.12	216	1.35×10^{-16}	1.8
9	15.13	64	1.70×10^{-16}	2.3
10	15.13	216	8.67×10^{-17}	2.7
11	15.70	125	1.66×10^{-16}	5.2
12	15.97	64	6.47×10^{-17}	17.7
13	22.29	125	5.91×10^{-16}	1.4
14	29.50	125	1.18×10^{-16}	0.16
15	29.56	125	6.82×10^{-15}	0.07
16	29.57	216	3.16×10^{-14}	0.01
17	30.40	125	1.56×10^{-14}	0.06

in describing the dynamics of coagulation of colloids. In previous reports [1,45,50,51] we have shown how ESS based on BD can incorporate the details of surfactant adsorption on emulsion stability. Here we used the same methodology to evaluate the coagulation constants of simple systems spanning a wide range of volume fractions with different degrees of polydispersity.

First, the thermal interaction between the solvent and the particles was addressed. It was found that the magnitude of the thermal exchange does not influence the flocculation constant sensibly for volume fractions lower than 0.15. In the absence of HI, a high value of U_T is required in order to reproduce the diffusion constants experimentally found. As shown by a simple estimation, a thermal exchange of considerable magnitude is likely to be experienced by a particle of few microns. It was noticed that such amount of energy could be enough for crossing the repulsive barrier between stabilized flocculated particles in a Brownian relaxation time, but this problem will be addressed in a future report.

According to these results, polydispersity can increase the value of the flocculation constant considerably. Combined changes in the volume fraction and the polydispersity of the system can increase k_f between one and two orders of magnitude. It was also found that the van der Waals interaction could increase the flocculation rate in at least one additional order of magnitude. However, preliminary results indicate that the introduction of HI may substantially slow down this increase producing values of the same order of magnitude as those originated by thermal exchange only.

Acknowledgements

This research was partially supported by the program " IVIC Founding for Applied Research" through grant 2000-23. Comments of Drs E. Dickinson and M. Whittle regarding the implementation of HI in BD simulations are very appreciated.

References

[1] Urbina-Villalba, G. and García-Sucre, M. (2000) "Brownian Dynamics simulation of emulsion stability", *Langmuir* **16**, 7975.
[2] von Smoluchowski, M. (1917) "Versuch einer mathematischen theorie der Koagulationskinetik kollider Lösungen", *Z. Phys. Chem.* **92**, 129.
[3] Verwey, E.J.W. and Overbeek, J.Th.G. (1999) *The Theory of Liophobic Colloids* (Dover, New York).
[4] Behrens, S.H., Borkovec, M. and Schurtenberger, P. (1988) "Aggregation in charge-stabilized colloidal suspensions revisited", *Langmuir* **14**, 1951.
[5] van den Tempel, M. (1953) "Stability of oil-in-water emulsions II. Mechanism of the coagulation of an emulsion", *Recueil* **72**, 433.
[6] Rice, C.L. and Whitehead, R. (1967) "The theory of the coagulation of emulsions", *J. Colloid. Interface Sci.* **23**, 174.
[7] Borwankar, R.P., Lobo, L.A. and Wasan, D.T. (1992) "Emulsion stability–kinetics of flocculation and coalescence", *Colloids Surf.* **69**, 135.
[8] Dhont, J.K.G. (1996) Chapters 5 and 3, *An Introduction to Dynamics of Colloids* (Elsevier Sicience B.V., Amsterdam).
[9] Batchelor, G.K. (1982) "Sedimentation in a dilute polydispersed system of interacting particles. Part 1. General Theory", *J. Fluid Mech.* **119**, 379.
[10] Batchelor, G.K. (1976) "Brownian diffusion of particles with hydrodynamic interaction", *J. Fluid Mech.* **74**, 1.
[11] Rotne, J. and Prager, S. (1969) "Variational treatment of hydrodynamic interaction in polymers", *J. Chem. Phys.* **50**, 4831.
[12] Honig, E.P., Roebersen, G.J. and Wiersema, P.H. (1971) "Effect of hydrodynamic interaction on the coagulation rate of hydrophobic colloids", *J. Colloid Interface Sci.* **36**, 97.
[13] Felderhof, B.U. (1977) "Hydrodynamic interaction between two spheres", *Physica A* **89**, 373.
[14] van de Ven, T.G.M. (1996) "Keeping pace with colloids in motion", *Langmuir* **12**, 5254.

[15] Tanaka, H. and Araki, T. (2000) "Simulation method of colloidal suspensions with hydrodynamic interactions: Fluid Particle Dynamics", *Phys. Rev. Lett.* **85**, 1338.
[16] Felderhof, B.U. (1978) "Diffusion of interacting Brownian particles", *J. Phys. A: Math Gen.* **11**, 929.
[17] Beenakker, C.W.J. and Mazur, P. (1982) "Diffusion of spheres in suspension: three-body hydrodynamic interaction effects", *Phys. Lett. A* **91**, 290.
[18] Medina-Noyola, M. (1988) "Long-time self-diffusion in concentrated colloidal dispersions", *Phys. Rev. Lett.* **60**, 2705.
[19] Pusey, P.N. and van Megen, W. (1983) "Measurement of the short-time self-mobility of particles in concentrated suspension. Evidence for many-particle hydrodynamic interactions", *J. Phy.* **44**, 285.
[20] Brown, J.C., Pusey, P.N., Goodwin, J.W. and Ottewill, R.H. (1975) "Light scattering study of dynamic and time-average correlations in dispersions of charged particles", *J. Phys. A* **8**, 664.
[21] Pusey, P.N. (1975) "The dynamics of interacting Brownian particles", *J. Phys. A* **8**, 1433.
[22] Pusey, P.N. (1978) "Intensity fluctuation spectroscopy of charged Brownian particles: the coherent scattering function", *J. Phys. A* **11**, 119.
[23] Pusey, P.N. (1982) "Langevin approach to the dynamics of interacting Brownian particles", *J. Phys. A* **15**, 1291.
[24] van Veluwen, A., Lekkerkerker, H.N.W., de Kruif, C.G. and Vrij, A. (1987) "Brownian diffusivities of interacting colloidal particles measured by dynamic light scattering", *Faraday Discuss Chem. Soc.* **83**, 59.
[25] Einstein, A. (1956) In: Fürph, R., ed, *Investigations on the Theory of Brownian Movement* (Dover Publications Inc., New York).
[26] Perrin, J. (1990) *Atoms* (Ox Box Press, Woodbridge).
[27] Vadas, E.B., Cox, R.G., Goldsmith, H.L. and Mason, S.G. (1976) "The microrheology of colloidal dispersions. II. Brownian diffusion of doublets of spheres", *J. Colloid Interface Sci.* **57**, 308.
[28] Beenakker, C.W.J. and Mazur, P. (1984) "Diffusion of spheres in a concentrated suspension II", *Physica A* **126**, 349.
[29] Satoh, A., Chantrell, R.W., Coverdale, G.N. and Kamiyama, S. (1998) "Stokesian dynamics simulations of ferromagnetic colloidal dispersions in a simple shear flow", *J. Colloid Interface Sci.* **203**, 233.
[30] Segre, P.N., Behrend, O.P. and Pusey, P.N. (1995) "Short-time Brownian Dynamics motion in colloidal suspensions: experiment and simulation", *Phys. Rev. E* **52**, 5070.
[31] Hoogerbrugge, P.J. and Koelman, J.M.V.A. (1992) "Simulating microscopic hydrodynamic phenomena with dissipative particle dynamics", *Europhys. Lett.* **19**, 155.
[32] Branka, A.C. (1999) "Algorithms for Brownian Dynamics computer simulations: multivariable case", *Phys. Rev. E* **60**, 2381.
[33] Whittle, M. and Dickinson, E. (1997) "Brownian Dynamics simulation of gelation in soft sphere systems with irreversible bond formation", *Mol. Physiol.* **90**, 739.
[34] Puertas, A.M., Fernández-Barbero, A. and de las Nieves, F.J. (1999) "Brownian Dynamics simulation of diffusive mesoscopic particle aggregation", *Comp. Phys. Comm.* **121**, 353.
[35] Nuesser, W. and Versmold, H. (1999) "Brownian Dynamics simulation of sedimented colloidal suspensions", *Mol. Physiol.* **96**, 893.
[36] Strating, P. (1999) "Brownian Dynamics simulation of hard-sphere suspension", *Phys. Rev. E* **59**, 2175.
[37] Oberholzer, M.R., Wagner, N.J. and Lenhoff, A.M. (1997) "Grand Canonical Brownian Dynamics simulation of colloidal adsorption", *J. Chem. Phys.* **107**, 9157.
[38] Dickinson, E. (1990) "Computer simulation of the coagulation and flocculation of colloidal particles", In: Bloor, D.M. and Wyn-Jones, E., eds, *The Structure, Dynamics and Equilibrium Properties of Colloidal Systems* (Kluwer Academic Press, The Netherlands) pp 707–727.
[39] Bacon, J., Dickinson, E. and Parker, R. (1983) "Motion of Flocs of two and three interacting colloidal particles in a hydrodynamic medium", *J. Chem. Soc. Faraday Trans 2*: **79**, 91.
[40] Dickinson, E. (1979) "Polydispersity and osmotic pressure of stable ordered colloidal dispersions", *J. Chem. Soc. Faraday Trans.* II, 466.
[41] Chen, J., Dickinson, E. and Iveson, G. (1993) "Interfacial interactions, competitive adsorption and emulsion stability", *Food Struct.* **12**, 135.
[42] Puertas, A.M., Maroto, J.A., Fernández-Barbero, A. and de las Nieves, F.J. (1999) "On the kinetics of heteroaggretion versus electrolyte concentration: comparison between simulation and experiment", *Colloids Surf. A* **151**, 473.
[43] Puertas, A.M. and de las Nieves, F.J. (1999) "Colloidal stability of polymer colloids with variable surface charge", *J. Colloid Interface Sci.* **216**, 221.
[44] Romero-Cano, M., Puertas, A.M. and de las Nieves, F.J. (2000) "Colloidal aggregation under steric interactions: simulation and experiments", *J. Chem. Phys.* **112**, 8654.
[45] Urbina-Villalba, G. and García-Sucre, M. (2001) "Influence of surfactant distribution on the stability of oil/water emulsions towards flocculation and coalescence", *Colloids Surf. A: Phys-Chem. Eng. Asp.* **190**, 111.
[46] Ermak, D. and McCammon, J.A. (1978) "Brownian Dynamics with hydrodynamic interactions", *J. Chem. Phys.* **69**, 1352.
[47] Chandrasekhar, S. (1943) "Stochastic problems in physics and astronomy", *Rev. Mod. Phys.* **15**, 1.
[48] Reif, F. (1965) Chapter 15, *Fundamentals of Statistical and Thermal Physics* (McGraw-Hill, New York) pp 574–577.
[49] Press, W.H., Teukolsky, S.A., Vetterling, W.T. and Flannery, B.P. (1999), Chapter 7, *Numerical Recipes in Fortran 77* (Cambridge University Press, New York) Vol. 1, pp 279–287.
[50] Urbina-Villalba, G. and García-Sucre, M. (2000) "Effect of non-homogeneous spatial distributions of surfactants on the stability of high-content bitumen-in-water emulsions", *Interciencia* **25**, 415.
[51] Urbina-Villalba, G. and García-Sucre, M. (2000) "A simple computational technique for the systematic study of adsorption effects in emulsified systems. Influence of Non-homogeneous surfactant distributions on the coalescence rate of a bitumen-in-water emulsion", *Mol. Simul.* **27**, 75.
[52] Allen, M.P. and Tildesley, D.J. (1987) *Computer Simulation of Liquids* (Oxford University Press).
[53] Hütter, M. (1999) "Coagulation rates in concentrated colloidal suspensions studied by Brownian dynamics simulation", *Phys. Chem. Chem. Phys.* **1**, 4429.
[54] Sonntag H., Strenge K (1987). "Coagulation kinetics and structure formation", VEB Deutscher Verlag der Wissenschaften, Berlin
[55] Holthoff, H., Schmitt, A., Fernández-Barbero, A., Borkovec, M., Cabrerízo-Vílchez, M.A., Schurtenberger, P. and Hidalgo-Alvarez, R. (1997) "Measurement of absolute coagulation rate constants for colloidal particles: comparison of single and multiple light scattering techniques", *J. Colloid Interface Sci.* **192**, 463–470.
[56] Bacon, J., Dickinson, E. and Parker, R. (1983) "Simulation of particle motion and stability in concentrated dispersions", *Faraday Discuss Chem. Soc.* **76**, 165.
[57] Fuchs, N. (1934) "Über der stabilität und aufladung der aerosole", *Z. Physik.* **89**, 736.